Recycling of iron and aluminum from drinking water treatment sludge for synthesis of a magnetic nanosorbent (ALCS-Al-Fe) to remove fluoride from drinking water

Feng Jing[1], Bai Hui[1], Han Yiwen[1],Zhang Rui[3], Zhu Puli[1], Bu Duo[2], Dan Zeng[2], Li Wei[2], Lu Xuebin[1,2]

[1]School of Environmental Science and Engineering, Tianjin University, Tianjin 300072, China

[2] Department of Chemistry and Environmental Science, School of Science, Tibet University, Lhasa 850000, China

[3] School of environmental and municipal engineering , TianJin ChengJian university, Tianjin 300384, China

Abstract: More attention has been paid to the deterioration of water bodies polluted by drinking water treatment sludge (DWTS) in recent years. In this study, a novel investigation for recovery of Al and Fe from DWTS has been conducted, which are used for the synthesis of a magnetic nanosorbent (ALCS-Fe-AL) by loading Al/Fe oxides onto acid leaching carbonized sludge (ALCS). And the low-cost magnetic adsorbent which can be easily separated from water by a magnet was tested for the ability to remove fluoride from drinking water. Key factors, including the content of Fe and Al in the adsorbent, adsorbent dosage and initial pH of aqueous solution, were investigated. The results showed that ALCS-Fe-AL (ALCS:Fe=3:3 & ALCS-Fe:Al=3:6, mass ratio) can remove 97.17% F^- (initial concentration is 10 mg/L) at pH=7, T=25°C and adsorbent dosage of 3.0 g/L. The absorbent could reduce the fluoride concentration to below 1.0 mg/L in drinking water which meets the level of drinking water standard recommended by the World Health Organization (WHO). In addition, it had a high selectivity for fluoride versus common co-existing ions and high fluoride removal efficiency in a wide range of initial pH of 4 – 9. At neutral initial pH, the adsorption isotherm was well fitted with the Langmuir model, and the maximum adsorption capacity reached a high value of 30.49 mg/g. The adsorption kinetics followed a pseudo-second order model. These properties showed that the ALCS-Fe-AL is a promising adsorbent for fluoride removal from drinking water.

Keywords: drinking water treatment sludge, nanosorbent, fluoride removal

1. Introduction

The waterworks produce large amounts of drinking water treatment sludge (DWTS) every day. With the increase of water consumption, the production of sludge will become larger and larger. How to dispose the massive drinking water treatment sludge has become an urgent problem to be solved. Due to the presence of organic pollutants, heavy metals and other harmful substances in the sludge, it exerts tremendous pressure on the environment. Therefore, increasingly importance has been attached to the minimization of sludge volume and the recycling of sludge (Zhou et al., 2015). In addition, due to the use of iron salts and aluminum salts as coagulants in the water treatment process, there are a great quantity of heavy metals (Al^{3+}, Fe^{3+}, Ca^{2+} and Mg^{2+}) in the drinking water treatment sludge (Zou et al., 2012). What's more, the sludge can be widely used as a biochar and be modified by salts to be a low-cost and effective adsorbent (Fan et al,. 2017; Feng et al,. 2018). Furthermore, the inorganic components in the sludge can be extracted by acid leaching and other methods, which can also significantly improve the performance of sludge carbon (SC) (Zou et al., 2012). Consequently, it is effective and feasible to prepare a novel adsorbent by using the modified sludge and the inorganic metal retained in the sludge, which can also fully utilize the DWTS.

As the demand for purified water continues to increase to meet the needs of a growing population, especially in developing countries, the removal of fluoride from drinking water has become an increasingly important issue of public concern. In 25 countries around the world, fluorosis plagues local people as a local public health problem and induces various diseases (Vithanage et al., 2015). The Guidelines for Drinking Water Quality as defined by

the WTO indicate that the fluoride content in drinking water should not exceed 1.50 ppm (Edition., 2011). Adsorption is considered to be one of the most promising fluoride removal technologies in terms of cost, design and operability (Mohapatra et al., 2009). For many years, alumina and aluminum-based adsorbents have been effective and important materials for researchers in the field of fluorine removal in water and wastewater (Du et al., 2014; Yami et al., 2015; Goswami et al., 2012). Besides, the nanoparticle (NP) is considered to be excellent adsorbents for fluoride removal. And it has become a hot topic of recent research due to its high reactivity, small size, excellent catalytic activity, high surface area, easy separation and many adsorption active sites (Dhillon et al., 2015; Zhang et al., 2014). Compared to other available conventional techniques, magnetic separation is regarded as an effective technique because of its simplicity, easy separation and operation. (Shirsath et al., 2015; Sivashankar et al. 2014). Moreover, due to the good magnetic separability, cost-effective nature, chemical consistency and positive environmental impact, adsorbents containing metal oxides or hydroxides, such as aluminum-based materials (Liu et al., 2016; Prathna et al., 2018) and iron oxide-based adsorbents (Kuang et al., 2017; Adak et al., 2017), become effective materials for the adsorption of fluoride (Dhillon et al., 2017). Therefore, it is feasible to load nano-aluminum and nano-iron on the sludge carbon to remove fluoride from drinking water.

The purpose of this study is to combine carbonized sludge with iron and aluminum salts extracted from the sludge and nano-sized to obtain a new magnetic nano-adsorbent the ALCS-Fe-Al for fluoride removal in drinking water : (1) Through a series of experiments, the most effective adsorbent and optimal adsorption conditions were explored to be used for the removal of fluoride in water under normal conditions. (2) In addition, the adsorption process of the adsorbent was explored by means of model establishment. (3) The adsorption performance, composition and adsorption mechanism of the adsorbent can be proved by SEM, BET, VSM, XRD and XPS. It can not only realize the recycling of sludge, but also provide a new method for the removal of fluoride in aqueous solution.

2. Materials and methods

2.1 Chemicals

Drinking water treatment sludge (DWTS, Tianjin, China), Anhydrous NaAC (Fuchen (Tianjin) Chemical Reagent Co., Ltd., China), PEG-4000 (Tianjin Kemiou Chemical Reagent Co., Ltd., China), Ethylene glycol (Tianjin Kemiou Chemical Reagent Co., Ltd., China), NaF (a fluoride standard solution, 1000ppm, Shanghai Anpu Experimental Technology Co., Ltd., China), HCl (Tianjin Yuanli Chemical Co., Ltd., China), NaOH (Tianjin Jiangtian Chemical Technology Co., Ltd., China), NaCl (Tianjin Dechuan Technology Co., Ltd., China) , $NaHCO_3$ (Tianjin Jiangtian Chemical Technology Co., Ltd., China), Na_2CO_3 (Tianjin Guangfu Technology Development Co., Ltd., China), Na_2SO_4 (Kematte (Tianjin) Chemical Technology Co., Ltd., China), $Na_3PO_4{\cdot}9H_2O$ (Tianjin Guangfu Fine Chemical Research Institute, China), Na_2SiO_3 (Tianjin Komio Chemical Reagent Co., Ltd., China). All chemicals are analytical grade and can be used without further purification.

2.2 Extraction of raw materials and preparation of the adsorbent

Firstly, the DWTS was sufficiently ground into fine particles after being dried. The sludge-based carbon (SC) was obtained by roasting these sludge particles at 700 °C for 2 h while being placed in a tube furnace (TL1200, Tianjin Tianyi Technology Co., Ltd., China) under a nitrogen-filled condition. A mixture was obtained by mixing SC with HCl (2 $mol{\cdot}L^{-1}$, an acid leaching agent) at a mass ratio of 1:20 (g:mL). And then, it was acid immersed for 80 min with the aid of ultrasonic waves. The acid leaching solution and acid-leached carbonized sludge (ALCS) were obtained by filtering the mixture.

Next, $Fe(OH)_3$ and $Al(OH)_3$ precipitates were obtained by adjusting the pH of the acid leaching solution at 6 and 13, respectively. And then, the obtained precipitates were respectively dissolved in an acid and then concentrated by heating to cool and crystallize to obtain $FeCl_3{\cdot}6H_2O$ and $Al_2(SO_4)_3{\cdot}18H_2O$, which were used as precursors for subsequent experiments.

Further, $FeCl_3{\cdot}6H_2O$ (0.81 g, 3.0 mmol), acid-leached carbonized sludge (ALCS, added in proportion), anhydrous NaAc (2.16 g) and PEG-4000 (0.60 g) were added to ethylene glycol (24.0 mL). The resulting mixture was then stirred and homogenized at room temperature and sonicated for 10 min. Next, the mixture was placed in a 50 mL Teflon-lined high temperature autoclave (IKA, Anhui Key Power Machinery Technology Co., Ltd., China) and reacted at 200 °C for 12 h (Deng et al., 2010). It can be taken out after being cooled to room temperature. After cross-rinsing several times with ethanol and distilled water, it was placed in a vacuum drying oven (DZF-6020, Kangheng Instrument Co., Ltd., China) and dried at 60 °C for 6 hours. Finally, the nano-iron-loaded ALCS-Fe can be obtained.

The ALCS-Fe obtained from the previous step and $Al_2(SO_4)_3 \cdot 18H_2O$ were placed in an aqueous solution of pH=6 in different ratios (Chai et al., 2013). After being thoroughly mixed and sonicated for 10 min, the mixture was placed in a constant temperature shaker at 80 °C for 4 h. And the whole process was carried out under nitrogen. It was separated from water by a magnet and dried in a vacuum drying oven at 60 °C for 6 h to prepare the ALCS-Fe-Al loaded with nano-iron-aluminum, which was used for the adsorption of fluoride in an aqueous solution.

2.3 Characterization

The microstructure and morphology of the ALCS-Fe-Al particles were examined by a scanning electron microscope (SEM, SIGMA 300, Beijing Oubo Optics Technology Co., Ltd., China). The composition of the adsorbent was identified by X-ray diffraction (XRD-6100, Shimadzu Enterprise Management Co., Ltd., China). The specific surface area of ALCS-Fe-Al was measured by nitrogen adsorption using a specific surface area analysis tester (BETA201A, Beijing Guanzheng Precision Electric Instrument Equipment Co., Ltd., China). The magnetic properties of the adsorbent were analyzed by a vibrating sample magnetometer (VSM, MPMS3, Quantum Design, USA). The chemical structure of the adsorbent before and after defluorination was determined by X-ray photoelectron spectroscopy (XPS, EscaLab 250Xi, Thermo Fisher, USA).

2.4 Adsorption performance

The adsorption performance of ALCS-Fe-Al particles was examined by batch experiment. A certain amount of adsorbent was added to the fluorine-containing solution (Initial fluoride concentration = 10 ppm, pH = 7, unless otherwise specified, the initial fluorine concentration and pH of the solution remained unchanged). The sample was then placed in a constant temperature shaker at 25 ° C until the adsorption reached equilibrium (unless otherwise stated, the temperature of the adsorption remained unchanged). The residual fluoride concentration in the aqueous solution was measured by a fluoride ion meter (PXSJ-216, Shanghai Yidian Scientific Instrument Co., Ltd., China) when the adsorption reached equilibrium. And then, the adsorption capacity and the fluoride removal rate were calculated. The equilibrium adsorption capacity (Qe, mg / g) is defined as the mass ratio of adsorbed fluoride to adsorbent. The fluoride removal rate (R, %) is defined as the percentage of fluoride adsorbed by the adsorbent to the initial fluoride concentration.

To investigate the effect of pH on adsorption, the initial pH of the fluoride solution was adjusted to a range of 4-9 using 0.01 M HCl or NaOH. The pH of the solution was measured by a pH meter (PHS-3C, Shanghai Yidian Scientific Instrument Co., Ltd., China). The initial fluoride concentration was set to 10 ppm. When the adsorption reached equilibrium, the concentration of residual fluoride in the solution was measured and the removal rate was calculated.

The effects of competitive coexisting anions on the adsorption of fluoride were investigated by adding NaCl, $NaHCO_3$, Na_2CO_3, Na_2SO_4, Na_3PO_4 and Na_2SiO_3 to the fluoride-containing solution. All chemicals are of analytical grade and could be used without further purification.

2.5 Regeneration

The adsorbent the ALCS-Fe-Al was collected by utilizing the magnetism of the magnet and used for regeneration and circulation. The organic solvent methanol was used as a desorbent to desorb the adsorbent for 5 h to achieve its regeneration. And then the desorbed adsorbent was used to carry out the experiment of adsorbing fluoride in the aqueous solution. In order to evaluate the reusability of the ALCS-Fe-Al, the adsorption efficiency of the adsorbent was measured in 6 regeneration cycles .

3. Results and discussion

3.1 Optimal conditions for fluoride removal with the the ALCS-Fe-Al

3.1.1 The effect of aluminum content in adsorbent

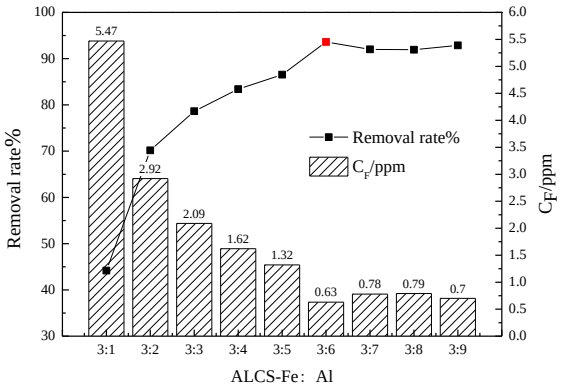

Fig.1. Effect of aluminum content in adsorbent: (a) ALSC: Fe = 1:1; (b) C_0 = 10 ppm; (c) adsorbent dosage = 2 g / L; (d) pH = 7; (e) T =25°C

Cai et al. used iron oxide/aluminum-loaded tea solid waste for the removal of fluoride ions. This experiment shows that the effect of aluminum in the adsorbent is significantly greater than that of iron (Cai et al., 2015). Therefore, This research first explore the effect of aluminum content in the adsorbent on the removal of fluoride in aqueous solution. As shown in the Fig.1, as the aluminum content in the adsorbent increased, the removal rate of fluoride in aqueous solution also increased sharply, which indicates that the aluminum content in the adsorbent has a great influence on the adsorption of fluoride. The removal rate of fluoride reached a maximum value with the ALCS-Fe:Al ratio of 1:2 (i.e., a mass ratio of ALCS-Fe:$Al_2(SO_4)_3$). As the aluminum content continued to increase, the fluoride removal rate remained essentially constant, indicating that the amount of aluminum supported in the adsorbent was saturated. The removal rate of fluoride can reach 93.6%, and the residual fluoride ion content in the aqueous solution is 0.63ppm, which meets the standard of safe drinking water.

3.1.2 The effect of iron content in adsorbent

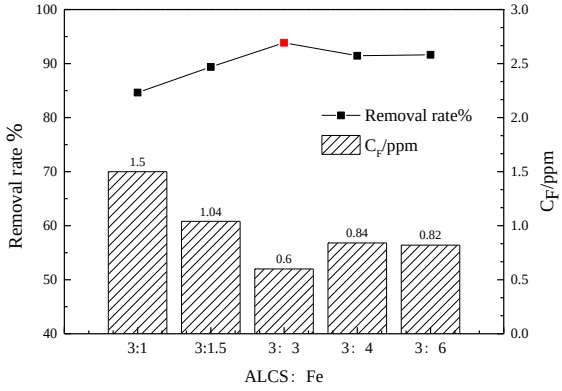

Fig.2. Effect of iron content in adsorbent: (a) ALSC-Fe:Al = 1:2; (b) C_0 = 10 ppm; (c) adsorbent dosage = 2 g / L; (d) pH = 7; (e) T =25°C.

The effect of iron content in the adsorbent was investigated while the ALCS-Fe:Al ratio was maintained at 1:2. As shown in the Fig. 2, as the iron content in the adsorbent increased, the removal rate of fluoride increased gradually. When the ratio ALCS:Fe (i.e., a mass ratio of ALCS : $FeCl_3 \cdot 6H_2O$) was increased to 1:1, the removal rate reached a maximum of 93.85% and the residual fluoride content in the aqueous solution was 0.60 ppm. By comparing the difference in the effect of the adsorbent on the adsorption of fluoride, which is caused by the different contents of iron and aluminum, it is worth mentioning that the effect of changes in aluminum content in the adsorbent is significantly greater than that of iron. Consequently, the addition of aluminum or sulfate to the

adsorbent can significantly enhance its adsorption of fluoride (Chai et al., 2013). Through the above investigation, the optimal preparation conditions of the adsorbent are determined: ALCS: Fe = 1:1 & ALCS-Fe: Al = 1:2. And we used the adsorbent prepared under this condition for the next study.

3.1.3 The effect of adsorbent dosage

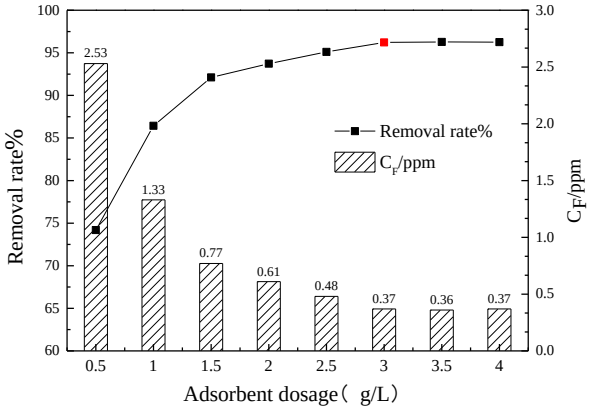

Fig.3. Effect of adsorbent dosage: (a) ALCS:Fe=1:1 & ALCS-Fe:Al=1:2; (b) C_0 = 10 ppm; (c) pH = 7; (d) T =25°C.

As shown in the Fig. 3, as the amount of adsorbent increased, the removal rate of fluoride in the adsorbent increased significantly, which indicates that the increase in the amount of biosorbent can provide sufficient surface active sites to adsorb fluoride in aqueous solution (Yu et al., 2013).When the amount of the adsorbent exceeded 3 g/L, the fluoride removal rate reached a maximum of 96.2%. The removal rate of the adsorbent was not changed much even if more adsorbent were added, which may be due to the fact that although the amount of the adsorbent is high, the residual fluoride concentration in the aqueous solution is low (Bansiwal et al., 2009).Therefore, 3g/L of the ALCS-Fe-Al was determined as the optimum adsorption amount for fluoride removal.

In summary, in the neutral aqueous solution with an initial fluoride ion concentration of 10 ppm, the optimum conditions for the removal of fluoride on the ALCS-Fe-Al are: ALCS: Fe = 1:1 & ALCS-Fe: Al = 1:2; adsorbent dosage = 3g / L. In fact, approximately 224 mg Fe (i.e., 4.0 mM) and 78 mg Al (i.e., 3.0 mM) can be extracted from 1 g carbonized sludge. According to this fact, a ALCS-Fe-Al* was obtained based on this preparation condition: ALCS: Fe = 1:1 & ALCS-Fe: Al = 2:1. Next, 3 g/L of the prepared ALCS-Fe-Al* was used for the removal of fluoride in a neutral aqueous solution with an initial fluoride ion concentration of 10 ppm.The fluoride removal rate can reach 86.7%, and the residual fluoride ion concentration is 1.31 ppm< 1.50 ppm, which is still able to meet the drinking water quality standard .

3.2 Adsorption and regeneration characterization of ALCS-Fe-Al

3.2.1 Adsorption isotherm

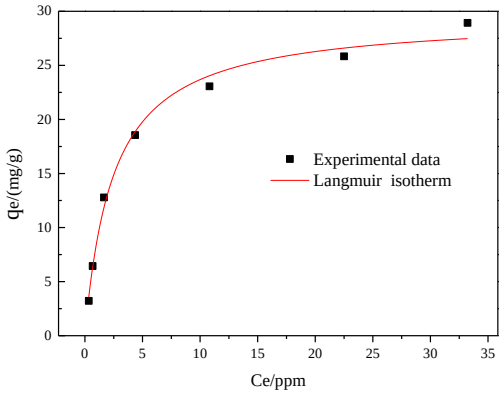

Fig.4. Adsorption isotherm on the ALCS-Fe-Al: (a) ALCS:Fe=1:1 & ALCS-Fe:Al=1:2; (b) C_0 = 10 ppm; (c) adsorbent dosage = 3 g / L; (d) pH = 7; (e) T =25°C.

Table 1. Langmuir and Freundlich isotherm parameters for adsorption of fluoride.

Adsorbent	The Langmuir isotherm model			The Freundlich isotherm model		
	q_m(mg/g)	K_L(L/mg)	R^2	K_F(mg/g)	n(g/L)	R^2
ALSC-Fe-Al	30.49	0.3523	0.9965	7.4456	4.2181	0.9108

The adsorption isotherm model is used to study the interaction and adsorption mechanism between solid adsorbent materials and adsorbate. At present, the two adsorption isotherms are used most widely : the Langmuir isotherm model and the Freundlich isotherm model, which can be used to predict the type of adsorption of ions on the adsorbent. The Langmuir isotherm model illustrates single-layer adsorption at the active site of the adsorbent (Ali et al., 2018), while the Freundlich isotherm model assumes that the adsorbent surface is not uniform, the adsorption capacity of each adsorption site is unequal, and there is an interaction between the adsorbed species (Lalley et al., 2016). The Langmuir and Freundlich isotherm models are mathematically expressed as follows:

The Langmuir isotherm model: $$q_e = \frac{K_L q_m C_e}{K_L C_e + 1} \quad (1)$$

Where q_e is the amount of adsorbed fluoride in equilibrium (mg/g); q_m is the maximum adsorption capacity for fluoride (mg/g); Ce is the concentration of fluoride at equilibrium (mg/L); K_L is the Langmuir equilibrium constant (L/mg).

The Freundlich isotherm model: $$q_e = K_F C_e^{\frac{1}{n}} \quad (2)$$

Where K_F is the isothermal constant for the Freundlich adsorption capacity (mg/g); n is the adsorption strength for the Freundlich isotherm (L/g).

By comparison, the Langmuir isotherm model (R^2 = 0.9965; Table 1) is more suitable for describing the adsorption process of fluoride on the ALCS-Fe-Al adsorbent than the Freundlich isotherm model (R^2=0.9108; Table 1). Therefore, the fluoride is adsorbed by the adsorbent through the single-layer surface adsorbent, indicating that the active site of the nanomaterial supported on the adsorbent plays an important role in the adsorption of fluoride (Cai et al., 2015). The q_e is plotted against Ce as shown in the Fig. 4. The adsorption process of the adsorbent adsorbing fluoride is in good agreement with the Langmuir model isotherm, and the maximum adsorption amount q_m is 30.49 mg/g.

3.2.2 Adsorption kinetics

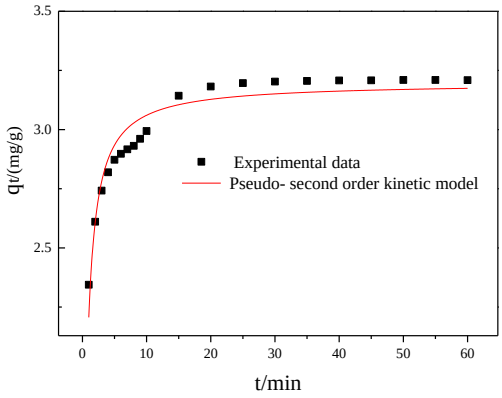

Fig.5. Adsorption kinetics on the ALCS-Fe-Al: (a) ALCS:Fe=1:1 & ALCS-Fe:Al=1:2; (b) C_0 = 10 ppm; (c) adsorbent dosage = 3 g / L; (d) pH = 7; (e) T =25°C.

Table 2. Lagergren pseudo-first-order and pseudo-second-order kinetic parameters for adsorption of fluoride.

Adsorbent	*qe.Exp.* (mg /g)	The pseudo-first-order kinetic model			The pseudo-second-order kinetic model		
		k_1(min^{-1})	*qe* (mg/g)	R^2	k_2 (g/mg/min)	*qe* (mg/g)	R^2
ALSC-Fe-Al	3.2095	0.1338	3.6033	0.9636	0.6120	3.2425	0.9998

We can predict the adsorption rate and understand the mechanism of adsorption of fluoride through adsorption kinetics, which is one of the most important characteristics representing adsorption efficiency.In this study, two kinetic models, Lagergren pseudo-first-order kinetic model and Lagergren pseudo-second-order kinetic model, were used to describe the kinetics of sorbent adsorption of fluoride.

The pseudo-first-order kinetic model：

$$Log(q_e - q_t) = Logq_e - \frac{k_1}{2.303}t \quad (3)$$

The pseudo-second-order kinetic model：

$$\frac{t}{q_t} = \frac{1}{k_2 q_e^{\ 2}} + \frac{1}{q_e}t \quad (4)$$

Where q_e is the amount of arsenic adsorbed at equilibrium (mg/g); q_t is the amount of arsenic adsorbed at a certain moment (mg/g); k_1 and k_2 are the pseudo-first-order and pseudo-second-order reaction rate constants, respectively; t is reaction time (min).

In contrast, the pseudo-second-order kinetic model (R^2 = 0.9998; Table 2) is more suitable than the pseudo-first-order kinetic model (R^2 = 0.9636; Table 2) to describe the adsorption of fluoride on the the ALCS-Fe-Al adsorbent.The kinetics of the adsorbent adsorbing fluoride is in good agreement with the pseudo-second-order kinetic model (Fig.5). Due to the faster adsorption kinetics of smaller particles (Badruzzaman et al., 2004), the adsorption of fluoride ions was very fast in the first 5 minutes and then decreased. Finally, it took about 60 minutes for the adsorption to reach equilibrium.

3.2.3 The effect of competitive coexisting anions

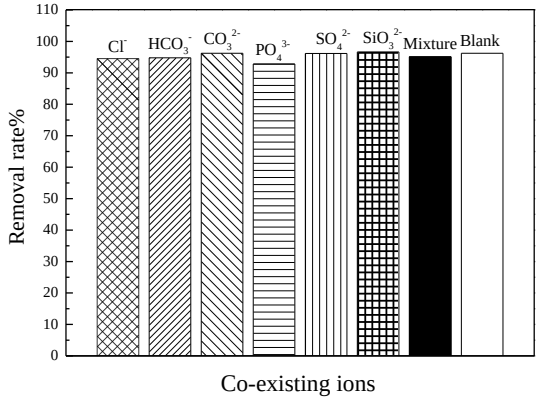

Fig.6. Effect of competitive coexisting anions on fluoride removal: (a) ALCS:Fe=1:1 & ALCS-Fe:Al=1:2; (b) C_0 = 10 ppm; (c) adsorbent dosage = 3 g / L; (d) pH = 7; (e) T =25°C.

In natural waters, other anions may compete with fluoride for adsorption sites, causing interference to adsorption and reducing sorbent removal efficiency (Dhillon et al., 2017). Therefore, this study selected typical anions (Cl^-, HCO_3^-, CO_3^{2-}, SO_4^{2-}, PO_4^{3-}, SiO_3^{2-}) in drinking water to explore the effect of coexisting anions on fluoride removal in water. And the ratio of the molar concentration of each ion in the water to the initial molar concentration of the fluoride ion was set to be 1:1.As shown in the Fig. 6, it can be observed that HCO_3^-, CO_3^{2-}, PO_4^{3-}, SiO_3^{2-} have no significant effect on fluoride adsorption.While Cl^- and SO_4^{2-} were present in the system, the amount of fluoride absorbed by the adsorbent from the aqueous solution was reduced.This may be due to a decrease in the partial adsorption sites of the fluoride, which is caused by the adsorption of Cl^- and SO_4^{2-} to specific adsorption sites on the surface of the magnetic nanoparticles, thereby forming competitive adsorption.However, in general, the presence of other coexisting anions in the water has little effect on the adsorption of F-, indicating that the adsorbent has a higher selectivity for the adsorption of fluoride and is suitable for fluoride removal in natural water environments.

3.2.4 Regeneration and circulation of the ALCS-Fe-Al

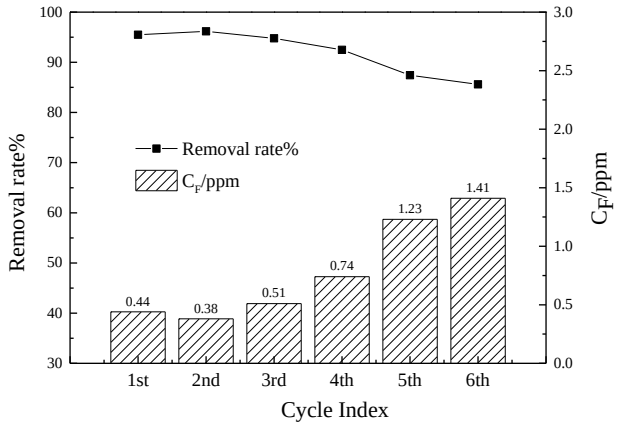

Fig.7. Regeneration and circulation of the ALCS-Fe-Al with methanol.

In order to evaluate the reusability of the ALCS-Fe-Al, the fluoride removal rates of the adsorbent were measured in 6 regeneration cycles using methanol as a desorbent. It can be seen from the Fig.7 that although the efficiency of the adsorbent to remove fluoride decreased with the increase of cycle times, the residual fluoride content in the water is 1.41 ppm after the adsorbent has been recycled for 6 times, which can still meet the standard

for safe drinking water. It also shows that methanol can regenerate the adsorbent effectively, which can be reused in a long period of time and still has a relatively high adsorption efficiency.

3.3 Characterization and adsorption mechanism of adsorbent

3.3.1 SEM

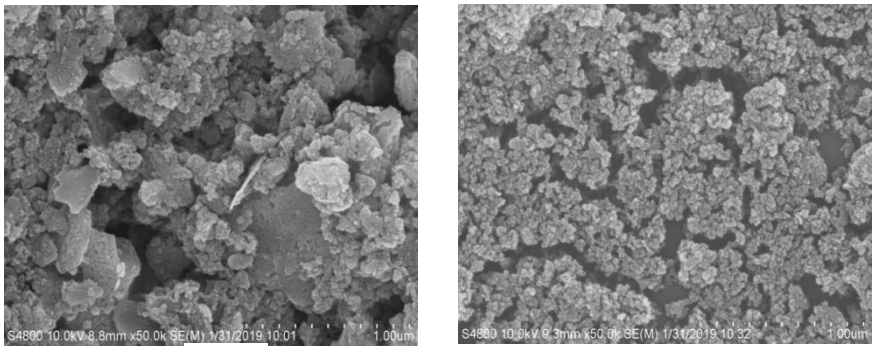

(a) (b)

Fig. 8. SEM images of the SC (a) and the ALCS-Fe-Al (b).

The SEM characterization results of the original sludge carbon (SC) and the prepared ALCS-Fe-Al are shown in the Fig.8. By comparing the two images, we can observe that SC has a smoother surface and more pores (Fig. 8. a), which can provide an attachment site and a larger surface area for the loading of the nanoparticles. In addition, the fact that the ALCS-Fe-Al loaded with nano-iron/aluminum has a relatively high BET specific surface area of 155.2 $m^2 \cdot g^{-1}$ also proves this. However, the surface of the the ALCS-Fe-Al adsorbent is relatively rough and is filled with spheroidal particles, indicating that the surface of the biochar has been loaded with nanoparticles after a series of preparation processes, which have high adsorption capacity, free active valence and surface energy (Dhillon et al., 2015). In addition, it can be seen from the Fig. 8. b that the nanoparticles have agglomeration on the surface of the biochar, which may be due to the higher surface energy and small size of the magnetic adsorbent.

3.3.2 VSM magnetic test

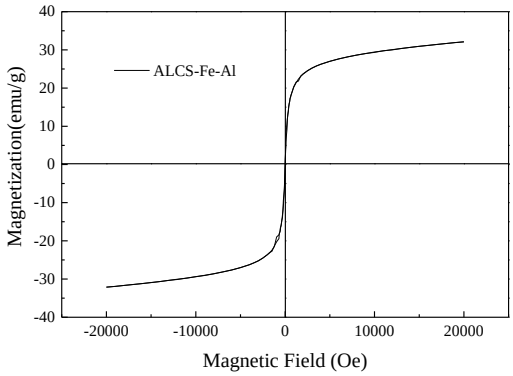

Fig. 9. Magnetic properties of the ALCS-Fe-Al.

The magnetization curve of the prepared the ALCS-Fe-Al is shown in the Fig. 9. We can observe that the magnetization increases with the increase of the strength of the applied magnetic field, and finally reaches the magnetic saturation. And the nano-adsorbent has a saturation magnetization of about 32.1 emu/g (1 emu/g = 1 $A \cdot m^2$ /kg). In addition, a magnetic adsorbent with a saturation value of 16.3 emu / g is sufficient to be separated from the water by a magnet (Ma et al., 2005).Therefore, the magnetic adsorbent can be separated and recovered from water by the magnetic properties of a magnet.

3.3.3 XRD

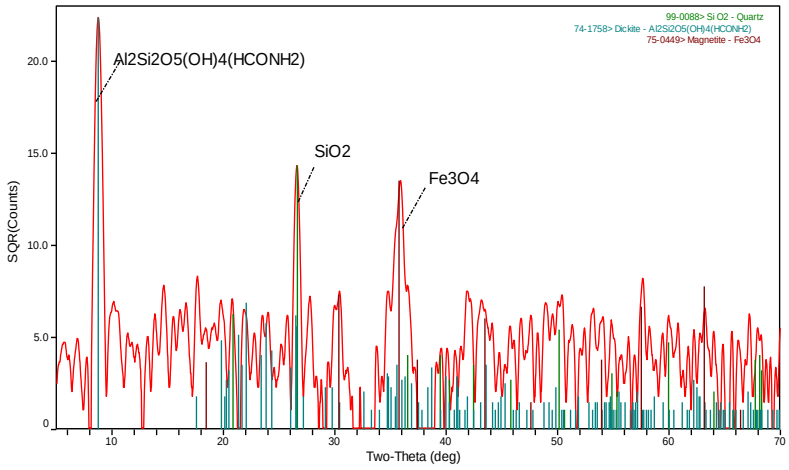

Fig. 10. XRD spectra of the ALCS-Fe-Al.

The XRD data of the ALCS-Fe-Al was analyzed by the jade software after the background value was subtracted. As shown in the Fig. 10, by compared with the PDF-2004 standard card, the peak position and peak intensity of the tested the ALCS-Fe-Al are substantially matched to the standard material. In addition, it can be observed that there are mainly three relatively strong diffraction peaks: The derivative peak at 2θ = 26.6° corresponds to the characteristic peak of SiO_2. This is due to the fact that the sludge-based carbon contains SiO_2, which may serve as a bonding point with nano iron and aluminum (Zarei et al., 2018; Zhang et al., 2018); The derivative peak at 2θ = 8.7° corresponds to the characteristic peak of $Al_2Si_2O_5(OH)_4(HCONH_2)$, which indicates that aluminum is likely to exist in the form of aluminum oxide or hydroxide in the adsorbent material, which can be combined with other elements such as C, O, and Si etc.. Further, the derivative peak at 2θ = 35.6°corresponds to the characteristic peak of the magnetic Fe_3O_4, which also explains that the adsorbent has a certain magnetic property. However, the state and type of Fe and Al present in the adsorbent can be further confirmed in conjunction with other characterization results and analysis.

3.3.3 XPS

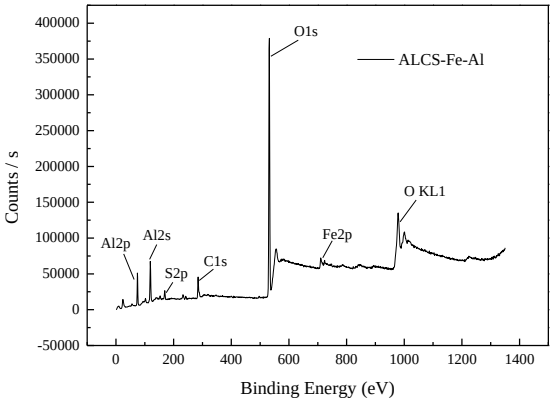

Fig.11. XPS full spectrum of ALCS-Fe-Al

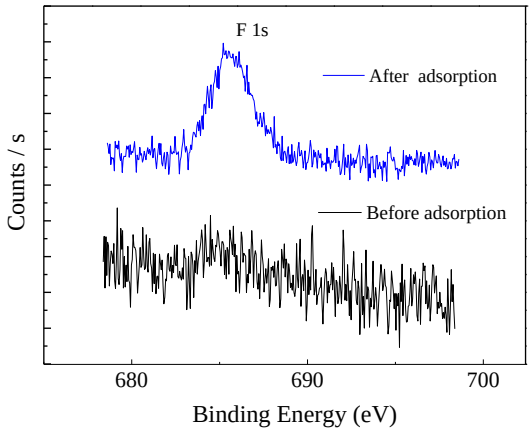

Fig.12. XPS spectra for F1s the ALCS-Fe-Al before adsorption and after adsorption.

Table 3. The binding energy (BE) and atomic concentration (AC) of the ALCS-Fe-Al before adsorption and after adsorption.

Name	Before adsorption		After adsorption		Atomic %	
	Peak BE (eV)	Assignments	Peak BE (eV)	Assignments	Before adsorption	After adsorption

Fe2p	710.57	Fe_3O_4	710.85	Fe_3O_4	1.61	1.49
F1s	-	-	685.18	Inorganic fluoride（Fe-F, Al-F, etc.）	0.00	1.33
O1s	531.74	-OH	531.74	-OH	58.53	54.25
C1s	284.97	C	284.89	C	12.83	17.48
S2p	169.07	SO_4^{2-}	168.93	SO_4^{2-}	2.86	2.44
Si2p	102.13	Si-O	102.06	Si-O	1.73	1.73
Al2p	74.36	Al_2O_3	74.34	Al_2O_3	22.45	21.28

As shown in the full spectrum of XPS of the ALCS-Fe-Al, the adsorbent mainly contains elements such as C, O, S, Si, Fe, and Al before adsorption (Fig. 11).

Moreover, by comparison with the standard XPS binding energy table, the binding energy of Fe2p peak (710.57 eV) and Al2p peak (74.36 eV) in the ALCS-Fe-Al correspond to Fe_3O_4 and Al_2O_3, respectively. Combined with the results of previous XRD characterization, it can be inferred that Fe_3O_4 and Al_2O_3 are present in the adsorbent.

In addition, the existence form and content of each element in the adsorbent before and after adsorption were comparatively analyzed, as shown in the table 3. An increase in the F element in the adsorbent after adsorption can be clearly seen, which can be more visually observed in the Fig. 12. And after adsorption, the binding energy of the F1s peak of ALCS-Al-Fe (685.18 eV) is significantly higher than that of NaF (684.5 eV), clearly indicating the reaction between the adsorbent and the fluoride (Wu et al., 2013).

Further more, the atomic ratio of each element of the adsorbent changed before and after adsorption: after the adsorbent adsorb fluoride, the atomic ratio of Fe2p, Al2p, O1s, S2p in the ALCS-Fe-Al decrease significantly, while the changes in F1s and C1s are reversed.Combined with the change in the binding energy of the peaks of these elements before and after adsorption, it can be inferred: (1) Fe-F and Al-F can be formed by the combination of Fe and Al with F by surface coordination of the adsorbent, and this was confirmed in many studies (Cai et al., 2015; Chai et al., 2013; Kuang et al., 2017). The reasons are as follows: Fe and Al are hard acids and have a higher valence state as a high-priced metal to provide an orbit for receiving electrons. While F^- is a hard base, which has a high electronegativity to provide electrons. According to the theory of hard and soft acids and bases, the two are easy to combine due to their strong affinity between them. (2) The decrease in the atomic ratio of S after adsorption indicates that SO_4^{2-} participates in the adsorption of F^- in water. And the removal of fluoride is the result of ion exchange through SO_4^{2-} and F^- (Chai et al., 2013). (3) It can also be seen that the atomic ratio of O1s is decreased, indicating that the -OH group is involved in the adsorption of fluoride. In fact, a part of the hydroxyl group is likely to be derived from sludge-based biochar. Many studies have shown that surface hydroxyl groups participate in the adsorption of fluoride in carbon-based adsorbents (Ajisha et al., 2015; Yu et al., 2015). In addition, the -OH group may also be derived from hydroxylated metal oxides. Because the metal oxide is easily hydrolyzed and hydroxylated in solution to form into $-M(OH)_X^{n-x}$ (Anderson et al., 1982). On the one hand, F^- can be adsorbed by ion exchange with OH^- in an acidic medium(Chen et al., 2016); On the other hand, if the potential of the surface of the particle is lower than the zero potential, the hydroxylated metal oxide is easily protonated to change its surface charge to be positive, thereby adsorbing the fluoride by electrostatic attraction (Jadhav et al., 2015).

3.3.4 The effect of the pH of the solution

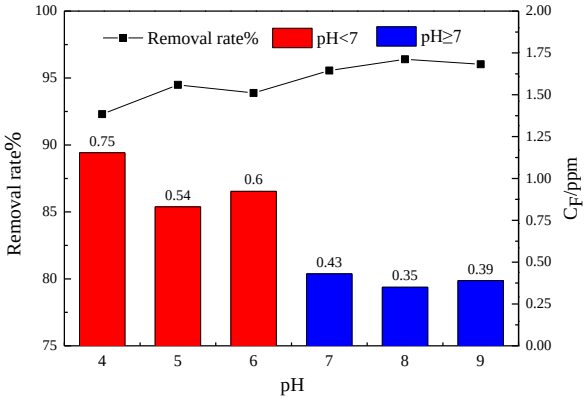

Fig.13. Effect of the pH of the solution on fluoride removal: (a) ALCS:Fe=1:1 & ALCS-Fe:Al=1:2; (b) C_0 = 10 ppm; (c) adsorbent dosage = 3 g / L; (d) T =25°C.

Table 4. The pH of aqueous solution before and after adsorption.

Before adsorption	4.00	5.00	6.00	7.00	8.00	9.00
After adsorption	5.76	6.06	6.28	6.18	6.18	6.24

As an important water chemistry parameter, the pH of the aqueous solution has a certain influence on the adsorption of fluoride.The 0.01 M HCl or NaOH was used to adjust the pH of the solution to a range of 4-9. The result shows that the ALCS-Fe-Al has a good removal effect on fluoride in water (Fig.13), which indicates that the adsorbent can be widely used in a wide pH range.

What's more, the surface of the solid particles in the solution will have different charges. According to the theory of electrostatic attraction, when the pH of the solution is higher than pHzpc (pH of zero point charge), the surface of the particle is negatively charged. Otherwise, it will be positively charged. However, a study has shown that (Lawrinenko et al., 2017) biochar mainly improves the pH at zero potential (pHzpc) by modifying the biochar with metal oxides or hydroxides, thereby increasing the anion exchange capacity and enabling it to be used in a wider pH range of the aqueous solution.Therefore,the pHzpc of the ALCS-Fe-Al mainly depends on the Fe_3O_4/Al_2O_3 contained therein. The pHzpc of Fe_3O_4/Al_2O_3 nanoparticles is 6.8 (Prathnaa et al., 2018), which indicates that the surface of the adsorbent has a positive charge in an aqueous solution under acidic conditions, while the surface of the adsorbent is negatively charged in a medium alkaline condition.However, we additionally observed changes in the pH of the solution before and after adsorption, as shown in the table 4. It can be seen that the pH value of the solution rised in the acidic medium after adsorption, while the pH value of the solution decreased in the neutral and alkaline medium after adsorption, which indicates that the adsorbent has a good buffering capacity in the adsorption process.This buffering effect can be explained by the amphoteric nature of the iron/aluminum oxide surface in the nanosorbent.According to the previous investigation of the mechanism of removing fluoride by this adsorbent, the metal oxides are easily hydrolyzed and hydroxylated in the solution (Anderson et al., 1982), resulting in the metal ions on the surface layer of the metal oxide having an unsaturated coordination. And the process of buffering the adsorbent can be expressed as follows (Zhang et al., 2016):

$$ALCS \equiv M^+ + OH^- \longleftrightarrow ALCS \equiv M - OH \quad (5)$$

$$ALCS \equiv M - OH + H^+ \longleftrightarrow ALCS \equiv M - OH_2^+ \quad (6)$$

$$ALCS \equiv M - OH + OH^- \longleftrightarrow ALCS \equiv M - O^- + H_2O \quad (7)$$

Where M represents the surface metal species; ALCS represents the acid-leached carbonized sludge.

As shown in the Fig.13, we can observe that the adsorption effect of the adsorbent on fluoride is stronger in neutral and alkaline media than in acidic media. Under acidic conditions, the adsorption may be based on electrostatic attraction; under alkaline conditions, as the pH of the solution increased, the zeta potential on the surface of the adsorbent decreased, which can weaken the electrostatic attraction of fluoride. Nevertheless, as shown in equation (8), hydroxylated metal oxides are prone to protonation in neutral and alkaline media if the potential of the surface of the particle is lower than the zero potential (Jadhav et al., 2015). When the effect is sufficient to change the surface charge to be positive, the fluoride can be adsorbed by the action of electrostatic attraction. Moreover, combined with XPS characterization analysis results, there is a surface coordination between high-valent metals (Fe, Al) and F with high electronegativity. Therefore, ligand exchange can be achieved by utilizing the surface coordination. The two mechanism occurred in two-step protonation / ligand exchange (Kuang et al., 2017):

$$ALCS \equiv M^{+} + H_2O \longleftrightarrow ALCS \equiv M - OH_2^{+} \quad (8)$$

$$ALCS \equiv MOH_2^{+} + F^{-} \longleftrightarrow ALCS \equiv M - F + H_2O \quad (9)$$

$$ALCS \equiv MOH + F^{-} \longleftrightarrow ALCS \equiv M - F + OH^{-} \quad (10)$$

Where M represents the surface metal species; ALCS represents the acid-leached carbonized sludge.

Although electrostatic adsorption can play a role in the adsorption process, the adsorption capacity increased with the increase of the pH in fluoride-containing sulotion, which indicates that electrostatic adsorption is not the main adsorption mechanism. Therefore, as a whole, the adsorption mechanism of the ALCS-Fe-Al to remove fluoride is mainly the result of simultaneous action of ligand exchange, surface coordination between the metal and F, electrostatic adsorption and ion exchange.

4. **Conclusion**

In this study, a novel nano-adsorbent (ALCS-Fe-Al) with magnetic separation for removing fluoride in drinking water was prepared by combining and nano-forming the acid-leached carbonized sludge (ALCS) with iron and aluminum salts extracted from the drinking water treatment sludge (DWTS). The adsorbent has good stability and high magnetic strength and is easily separated from the solution. The results show that the fluoride concentration of the fluoride-containing wastewater (10 ppm) can be reduced to less than 1.50 ppm by the adsorption of ALCS-Fe-Al, which meets the internationally prescribed drinking water quality standards. The kinetic study shows that the adsorption process of fluoride on ALCS-Fe-Al follows the Lagergren pseudo-first-order kinetic model. The adsorption isotherm is consistent with the Langmuir model, and the adsorption capacity is 30.49 mg/g. Furthermore, nano-Fe_3O_4/Al_2O_3 and abundant hydroxyl groups on the surface of ALCS-Fe-Al act as active sites for fluoride adsorption. And the adsorption mechanism of the adsorbent to remove fluoride is mainly the result of simultaneous action of ligand exchange, surface coordination, electrostatic adsorption and ion exchange. In addition, the adsorbent can be used in a wide range of pH = 4-9 and has a certain buffering capacity for changes in the pH of the solution. And the presence of aqueous anionic anions has a slight effect on the removal of fluoride on the ALCS-Fe-Al. Consequently, the nanoadsorbent can be widely applied to the removal of fluoride for drinking water. Moreover, The ALCS-Fe-Al can be easily and quickly regenerated with methanol as a desorbent, and the adsorption efficiency is still high after 6 regeneration cycles. This research not only provides a new way for the recycling of sludge, but also a new method for fluoride removal from drinking water.

5. Acknowledgement

Financial support of this study provided by Tibet University 2018 Central Financial Support Special Funds for Local Colleges and Universities ([2018] No. 54) and Cultivation Foundation of Tibet University (ZDTSJH18-04).

References

Adak, M. K., Sen, A., Mukherjee, A., Sen, S., Dhak, D., 2017. Removal of fluoride from drinking water using highly efficient nano-adsorbent, Al (III)-Fe (III)-La (III) trimetallic oxide prepared by chemical route. Journal of Alloys and Compounds, 719, 460-469.

Ajisha, M. A. T., Rajagopal, K., 2015. Fluoride removal study using pyrolyzed Delonix regia pod, an unconventional adsorbent. International Journal of Environmental Science and Technology, 12(1), 223-236.

Ali, M. E., 2018. Synthesis and adsorption properties of chitosan-CDTA-GO nanocomposite for removal of hexavalent chromium from aqueous solutions. Arabian Journal of Chemistry, 11(7), 1107-1116.

Anderson, M. A., Rubin, A. J., 1982. Adsorption of inorganics at solid-liquid interfaces. Soil Science, 133(4), 257-258.

Badruzzaman, M., Westerhoff, P., Knappe, D. R., 2004. Intraparticle diffusion and adsorption of arsenate onto granular ferric hydroxide (GFH). Water research, 38(18), 4002-4012.

Bansiwal, A., Thakre, D., Labhshetwar, N., Meshram, S., Rayalu, S., 2009. Fluoride removal using lanthanum incorporated chitosan beads. Colloids & Surfaces B Biointerfaces, 74(1), 216-224.

Cai, H. M., Chen, G. J., Peng, C. Y., Zhang, Z. Z., Dong, Y. Y., Shang, G. Z., Wan, X. C., 2015. Removal of fluoride from drinking water using tea waste loaded with Al/Fe oxides: A novel, safe and efficient biosorbent. Applied Surface Science, 328, 34-44.

Chai, L., Wang, Y., Zhao, N., Yang, W., You, X., 2013. Sulfate-doped Fe3O4/Al2O3 nanoparticles as a novel adsorbent for fluoride removal from drinking water. Water research, 47(12), 4040-4049.

Chen, L., Zhang, K., He, J., Cai, X. G., Xu, W., Liu, J. H., 2016. Performance and mechanism of hierarchically porous ce–zr oxide nanospheres encapsulated calcium alginate beads for fluoride removal from water. Rsc Advances, 6(43), 36296-36306.

Deng, H., Xiaolin, L. I. , Peng, Q., Wang, X., Chen, J., Yadong, L. I., 2010. Monodisperse magnetic single-crystal ferrite microspheres. Angewandte Chemie, 44(18), 2782-2785.

Dhillon, A., Kumar, D., 2015. Nanocomposite for the detoxification of drinking water: effective and efficient removal of fluoride and bactericidal activity. New Journal of Chemistry, 39(12), 9143-9154.

Dhillon, A., Prasad, S., Kumar, D., 2017. Recent advances and spectroscopic perspectives in fluoride removal. Applied Spectroscopy Reviews, 52(3), 175-230.

Du, J., Sabatini, D. A., Butler, E. C., 2014. Synthesis, characterization, and evaluation of simple aluminum-based adsorbents for fluoride removal from drinking water. Chemosphere, 101, 21-27.

Edition, F., 2011. Guidelines for drinking-water quality. WHO chronicle, 38(4), 104-8.

Fan, S. , Wang, Y. , Wang, Z. , Tang, J. , Tang, J. , Li, X., 2017. Removal of methylene blue from aqueous solution by sewage sludge-derived biochar: adsorption kinetics, equilibrium, thermodynamics and mechanism. Journal of Environmental Chemical Engineering, 5(1), 601-611.

Feng, M., Zhang, W., Wu, X., Jia, Y., Jiang, C., Wei, H., Tsang, D. C.,2018. Continuous leaching modifies the surface properties and metal (loid) sorption of sludge-derived biochar. Science of the total environment, 625, 731-737.

Goswami, A., Purkait, M. K., 2012. The defluoridation of water by acidic alumina. Chemical Engineering Research and Design, 90(12), 2316-2324.

Jadhav, S. V., Bringas, E., Yadav, G. D., Rathod, V. K., Ortiz, I., Marathe, K. V., 2015. Arsenic and fluoride contaminated groundwaters: a review of current technologies for contaminants removal. Journal of Environmental Management, 162, 306-325.

Kuang, L., Liu, Y., Fu, D., Zhao, Y., 2017. Feooh-graphene oxide nanocomposites for fluoride removal from water: acetate mediated nano feooh growth and adsorption mechanism. Journal of Colloid & Interface Science, 490, 259-269.

Kuang, L., Liu, Y., Fu, D., Zhao, Y., 2017. FeOOH-graphene oxide nanocomposites for fluoride removal from water: Acetate mediated nano FeOOH growth and adsorption mechanism. Journal of colloid and interface science, 490, 259-269.

Lalley, J., Han, C., Li, X., Dionysiou, D. D., Nadagouda, M. N., 2016. Phosphate adsorption using modified iron oxide-based sorbents in lake water: kinetics, equilibrium, and column tests. Chemical Engineering Journal, 284, 1386-1396.

Lawrinenko, M., Jing, D., Banik, C., Laird, D. A., 2017. Aluminum and iron biomass pretreatment impacts on biochar anion exchange capacity. Carbon, 118, 422-430.

Liu, L., Cui, Z., Ma, Q., Cui, W., Zhang, X., 2016. One-step synthesis of magnetic iron–aluminum oxide/graphene oxide nanoparticles as a selective adsorbent for fluoride removal from aqueous solution. RSC Advances, 6(13), 10783-10791.

Ma, Z., Guan, Y., Liu, H., 2005. Synthesis and characterization of micron-sized monodisperse superparamagnetic polymer particles with amino groups. Journal of Polymer Science Part A: Polymer Chemistry, 43(15), 3433-3439.

Mohapatra, M., Anand, S., Mishra, B. K., Giles, D. E., Singh, P., 2009. Review of fluoride removal from drinking water. Journal of environmental management, 91(1), 67-77.

Prathna, T. C., Raichur, A. M., 2018. Fluoride removal from aqueous solutions using poly(styrene sulfonate)/nanoalumina multilayer thin films. Global Challenges, 2(2), 1700064.

Prathnaa, T. C., Sitompula, D. N., Sharmaa, S. K., Kennedya, M., 2018. Synthesis, characterization and performance of iron oxide/alumina-based nanoadsorbents for simultaneous arsenic and fluoride removal. DESALINATION AND WATER TREATMENT, 104, 121-134.

Shirsath, D. S. , Shirivastava, V. S., 2015. Adsorptive removal of heavy metals by magnetic nanoadsorbent: an equilibrium and thermodynamic study. Applied Nanoscience, 5(8), 927-935.

Sivashankar, R. , Sathya, A. B. , Vasantharaj, K. , Sivasubramanian, V., 2014. Magnetic composite an environmental super adsorbent for dye sequestration – a review. Environmental Nanotechnology, Monitoring & Management, 1-2, 36-49.

Vithanage, M., Bhattacharya, P., 2015. Fluoride in the environment: sources, distribution and defluoridation. Environmental Chemistry Letters, 13(2), 131-147.

Wu, X., Zhang, Y., Dou, X., Zhao, B., Yang, M., 2013. Fluoride adsorption on an Fe–Al–Ce trimetal hydrous oxide: characterization of adsorption sites and adsorbed fluorine complex species. Chemical engineering journal, 223, 364-370.

Yami, T. L., Du, J., Brunson, L. R., Chamberlain, J. F., Sabatini, D. A., Butler, E. C., 2015. Life cycle assessment of adsorbents for fluoride removal from drinking water in East Africa. The International Journal of Life Cycle Assessment, 20(9), 1277-1286.

Yu, X., Tong, S., Ge, M., Zuo, J., 2013. Removal of fluoride from drinking water by cellulose@hydroxyapatite nanocomposites. Carbohydrate Polymers, 92(1), 269-275.

Yu, Y., Wang, C., Guo, X., Chen, J. P., 2015. Modification of carbon derived from Sargassum sp. by lanthanum for enhanced adsorption of fluoride. Journal of colloid and interface science, 441, 113-120.

Zhou, Z. , Yang, Y. , Li, X. , Zhang, Y. , Guo, X. , 2015. Characterization of drinking water treatment sludge after ultrasound treatment. Ultrasonics Sonochemistry, 24, 19-26.

Zarei, A., Saedi, S., 2018. Synthesis and Application of Fe3O4@ SiO2@ Carboxyl-Terminated PAMAM Dendrimer Nanocomposite for Heavy Metal Removal. Journal of Inorganic and Organometallic Polymers and Materials, 28(6), 2835-2843.

Zhang, C., Chen, L., Wang, T. J., Su, C. L., Jin, Y., 2014. Synthesis and properties of a magnetic core-shell composite nano-adsorbent for fluoride removal from drinking water. Applied Surface Science, 317, 552-559.

Zhang, C., Li, Y., Wang, T. J., Jiang, Y., Wang, H., 2016. Adsorption of drinking water fluoride on a micron-sized magnetic Fe3O4@ Fe-Ti composite adsorbent. Applied Surface Science, 363, 507-515.

Zhang, W., Zhang, S., Wang, J., Wang, M., He, Q., Song, J., Zhou, J., 2018. Hybrid functionalized chitosan-Al2O3@ SiO2 composite for enhanced Cr (VI) adsorption. Chemosphere, 203, 188-198.

Zou, J., Dai, Y., Tian, C., Pan, K., Jiang, B., Wang, L., Fu, H., 2012. Structure and properties of noncrystalline nano-Al(OH)3 reclaimed from carbonized residual wastewater treatment sludge. Environmental science & technology, 46(8), 4560-4566.